Proceedings Paper:
Jackson, M, Hunter, T orcid.org/0000-0003-3922-491X, Goode, J et al. (1 more author) (2020) Drying Wet Stored and Corroded Magnox Fuel for Interim Dry Storage. In: WM2020 Conference Proceedings: Reducing Long-Term Environmental Liability Through Efficient, Effective Clean-Up. WM2020: Waste Management Symposia, 08-12 Mar 2020, Phoenix, AZ, USA. WM Symposia . ISBN 978-0-9836186-4-5

Drying Wet Stored and Corroded Magnox Fuel for Interim Dry Storage – 20187

Matthew Jackson*, Timothy Hunter*, James Goode** and Bruce Hanson*
*School of Chemical and Process Engineering, University of Leeds
**National Nuclear Laboratory

ABSTRACT

To investigate the feasibility of drying corroded Magnesium alloy clad nuclear fuel, the corrosion products of inactive and unirradiated Magnox simulant dry corrosion product and dried corroded Magnox sludge were characterised by X-ray diffraction and thermogravimetric analysis. XRD identified brucite in the dried corrosion product and both brucite and hydromagnesite in the sludge. TGA identified mass loss on dehydration of ~9.1% up to 250 °C and 27.9% from dehydroxylation up to 440 °C, with total mass loss of 41.9% up to 800 °C for the dried corrosion product. The sludge TGA showed 8.3% mass loss up to 250 °C from dehydration, 7.5% up to 330 °C from dehydroxylation and 31.4% mass loss up to 47.2% for decarbonation, with total mass loss of 49.2% up to 800 °C. Water removal up to 1.8 g was performed by cold vacuum drying (40 °C-120 °C) on a ≈14.8 g (wet) corroded Magnox sample. The process was monitored by observing pressure, dew point, temperature and gas flow changes supported by measuring the sample mass loss as water is removed. From these tests, it was observed that the dried corroded Magnox displayed some hygroscopic capacity which has implications for water retention following vacuum drying and the length of exposure required to achieve the desired dryness. Whilst at higher temperatures the water was removed faster, the increased temperature also risks the fuel cladding undergoing unwanted chemical reactions with the residual water during the process. However, at lower temperatures the achievable levels of dryness were reduced. Therefore, from these observations this work has identified that there is a temperature balance that may be necessary to optimise the drying process with respect to allowing the greatest level of dryness whilst restricting unwanted chemical reactions.

INTRODUCTION

Nuclear fission has been used a source of electricity generation since the first reactor at Calder Hall in 1956 [1] and in 2017 accounted for 20.8% of electricity produced in the UK [2]. Currently all UK nuclear energy is produced by seven CO_2 cooled graphite moderated Advanced Gas-Cooled Reactor (AGRs) stations - the fuel for which consists of UO_2 pellets clad in stainless steel - and one Pressurised Water Reactor (PWR) station [3]. These reactors were preceded by a fleet of another type of gas cooled reactor known as Magnox reactors - the first commercial nuclear energy reactors built in the UK. The name "Magnox" is derived from the Magnesium Non-OXidising alloy which clad the uranium metal fuel rod. Energy has been produced by Magnox reactors up until the closure of the final UK Magnox reactor at Wylfa in 2015 [4].

Spent nuclear fuel is commonly stored under water in ponds following reactor operation to provide cooling and shielding while short lived fission products decay. A significant drawback to underwater storage of Magnox fuel is that both the Magnox cladding and the uranium metal fuel will react with the pond water. Over time this corrosion causes issues for several reasons; it complicates the handling of the fuel, the pond water becomes contaminated with radioactive material, the corrosion products produce secondary wastes which must be managed, and some corrosion products (particularly magnesium hydroxide) form a sludge which affects visibility when disturbed [5]. Long term storage of Magnox spent fuel has resulted in hazardous areas at Sellafield, particularly the First Generation Magnox Storage Pond (FGMSP) and Magnox Swarf Storage Silo (MSSS) which are now priority remediation projects in UK nuclear decommissioning [6].

It is important during wet storage of all types of nuclear fuel that water chemistry is controlled such that; metal surface corrosion is minimised, the concentration of radionuclides in the storage pond is kept as low as possible, and the water clarity is maintained to enable ease of inspection and operations. The corrosion of steel clad AGR fuel, and zirconium alloy clad LWR fuel is manageable with corrosion rates reported as low as 1×10^{-6} µm/a for zirconium alloy and 0.1 µm/a for stainless steel AGR cladding [5]. In order to reduce the corrosion of Magnox cladding during storage the ponds are maintained by dosing with sodium hydroxide to pH 11.5, and the presence of aggressive corrosion ions like Cl^- must be avoided as they can induce pitting corrosion. Aqueous storage of magnesium in pH 11.5 sodium hydroxide is known to form magnesium hydroxide and hydrogen according to Eq. 1:

Eq. 1 $$Mg + 2H_2O \rightarrow Mg(OH)_2 + H_2$$

The magnesium hydroxide produced from this reaction forms a protective layer which can slow further corrosion, but the protective film can also be dissolved by the presence of acidic species - hence the desire to store the spent fuel in alkaline conditions to preserve the protective hydroxide as shown in Eq. 2: [5]

Eq. 2 $$Mg(OH)_2 + 2H+ \rightarrow Mg_2+ + 2H_2O$$

Safe storage of Magnox fuel in water has been demonstrated for 5 years at pH ≥11.4 (dosed with sodium hydroxide) and maintaining chloride and sulphate ion content <1 ppm [5]. Friskney et al. [7] quote that etched Magnox at ambient temperature initially corrodes at an elevated rate, which decreases over a period of days to the 'constant' rate of ~0.01 mg dm^{-2} d^{-1}. At higher temperatures, this initial period of increased corrosion rate transitions more swiftly to the 'constant' rate. After a period of time at the 'constant' rate, the magnesium corrosion rate switches to a new constant but elevated 'post-breakaway' rate. The time for the sample to achieve 'breakaway' decreases with increasing temperature, and is ~120 hours at 100 °C. Friskney et al. state that the corrosion rate in pH 11.5 sodium hydroxide solution increases significantly with increasing temperature up to 100 °C [7]. On this basis it is clear that increasing the temperature significantly increases the pre- and post-breakaway Magnox corrosion rates.

Wet storage is also common practice for AGR and Light Water Reactor (LWR) spent fuel, and the cladding of these fuel types is largely resistant to corrosion during wet storage, but alternative storage in dry conditions has also been employed. Removal of Magnox from underwater storage and performing drying could prevent unwanted further corrosion, enabling less hazardous and more manageable storage conditions. Dry storage of Magnox has been successfully implemented in the UK at Wylfa Power Station in Wales, where the spent Magnox fuel is discharged from the reactor straight into CO_2 filled dry storage pending transport to Sellafield for reprocessing, not in a water cooled pond like at most other sites [8]. Carbon dioxide is well suited for dry storage as Magnox corrosion rates in CO_2 are negligible at temperatures <350 °C and feasible in dry air at <150 °C, but will undergo pitting if the relative humidity exceeds 50% or if water ingress occurs [5]. This shows there is demonstrated viability for dry storage of Magnox spent fuel. Drying of previously wetted and/or corroded Magnox fuel has been considered in the past but has not been thoroughly investigated or demonstrated [9]. The 2015 Office for Nuclear Regulation (ONR) review considers drying the fuel as a contingency, estimating 4.5-6.5 years for deployment, followed by 1-4 years of operations depending on the outstanding Magnox inventory. This has the potential to result in fuel ageing for an additional 5.5-10.5 years in pond storage [10].

Vacuum drying is an established treatment for nuclear material, and common practices can typically involve performing a "rebound test" by evacuating below a set pressure limit, isolating the system and holding below the set pressure for a given amount of time (defined as 4 mbar over 30 minutes by ASTM C1553-16) [11]. Goode et al. observed dryness by directly measuring the presence of moisture and water vapour from dew point, mass flow, pressure and temperature, [12] which is advantageous as it does not rely on the low operating pressure or waiting for pressure rises, however application of this technique to

corroded Magnox fuel is novel. Corroded Magnox fuel has more avenues for water retention than AGR fuel via corrosion product porosity and chemical interaction, as well as the significantly greater corrosion rate Magnox experiences in water as discussed previously. This investigation looks to investigate and demonstrate the feasibility of transitioning Magnox spent fuel from wet to dry storage, and test how Magnox cladding and corrosion affects drying efficacy. Water may be held physically or chemically and the extent of these interactions must be understood if a drying regime is to be adopted industrially. The presence of water during storage can lead to further chemical reactions with fuel and cladding, as well as radiolysis. In order to support the industrial application of Magnox spent fuel drying it must be proven that Magnox fuel can be adequately dried to stop these reactions occurring in interim storage.

METHODOLOGY

Sample Preparation

Three corroded Magnox samples were used for characterisation and vacuum drying tests, all of which were supplied and previously corroded by the National Nuclear Laboratory and shown below in Figure 1a-c. Test material from Sample 1 was prepared by scraping dried corrosion product from the surface of a piece of an as received corroded Magnox can fragment. Sample 2 was prepared by 30 °C ultrasonic treatment of a piece of corroded Magnox for 9 hours, which caused the white corrosion product to be removed from the metal surface and fall to the bottom as a white sludge. The resultant corroded Magnox sludge was collected and dried overnight at 40 °C, yielding the fine grey powder used for analysis and characterisation.

Sample 3 consists of an as received corroded Magnox can fragment to investigate the drying behaviour of the wet Magnox. The surface of the whole sample is covered with a layer of white corrosion product. It is 70 mm tall, with 12 fins are along the whole length. The fins are bent and deformed, with four fins extending 35 mm from the beyond the top of the fragment. Between the fins a build-up of white corrosion product is visible.

a) Sample 1 b) Sample 2 c) Sample 3

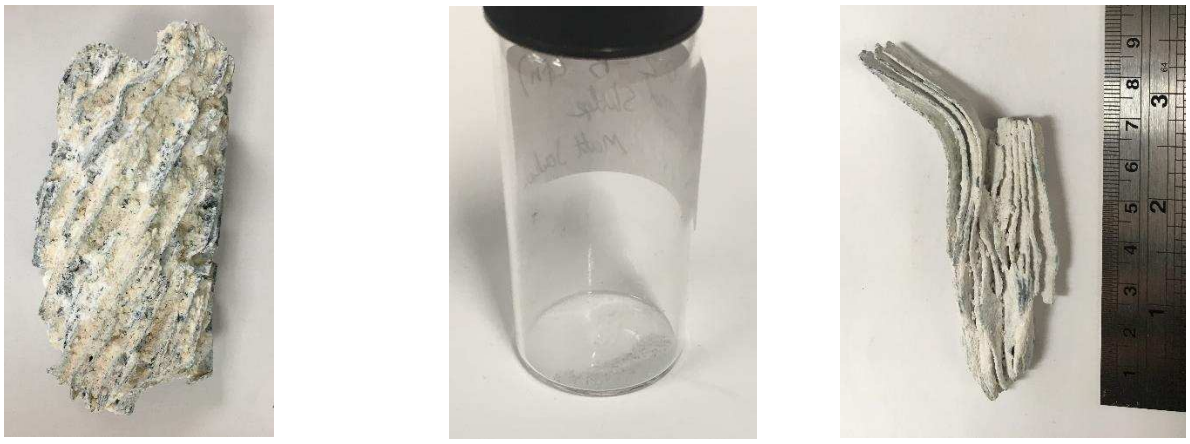

Figure 1. Corroded Magnox Test Samples; a) Sample 1 Corroded Magnox, b) Sample 2 Dried Sludge, c) Sample 3 Corroded Magnox for Vacuum Drying Tests

X-Ray Diffraction and Thermogravimetric Analysis

X-Ray Diffraction (XRD) analysis was performed on Sample 1 and 2 using a Malvern PAnalytical X'Pert Pro MPD X-ray diffractometer on 20-30 mg of scraped corrosion product and dried sludge. Thermogravimetric analysis (TGA) was undertaken on 19.62 mg Sample 1 and 13.33 mg Sample 2 using a Mettler Toledo TGA/DSC1, with exhaust sampling by a Nicolet Thermo iS10 FT-IR spectrometer, operated under a flow of 50 mL/min with an initial 15 min purge, followed by a 10 °C/min ramp from 30 to 800 °C.

Vacuum Drying

A drying rig was assembled at the University of Leeds and is shown in Figure 2. [13] It consists of various components which allow control and monitoring of the drying conditions, which are described below. Before undertaking drying tests the operational capabilities of the rig were assessed to ensure it could operate and perform consistently by achieving and holding suitably reduced pressure maintaining constant temperature and providing appropriate data for analysis.

The rig consists of a vessel with a bolt mounted flange, sealed with various ports for gas flow and monitoring of vessel conditions. A band heater is installed around the vessel which allows elevated temperatures to be achieved and is controlled externally. Instrumentation to monitor the vessel pressure, temperature and dew point are inserted via sealed inlets to reduce leakages. The rig also has a gas flowmeter to observe the flow velocity during vacuum and flowed gas drying operations. Molecular sieves are present to capture evaporated water, allowing for water mass balance to be achieved as well as protecting the vacuum pump from taking in moisture. Pressures of 3-4 mbar are achievable in the current rig arrangement. The on-line logging instrumentation specification is as follows:

- Pressure - measured by an OMEGA PXM319-002A10V 0-2 barA pressure transducer, with voltage logged by TracerDAQ and converted using manufacturer supplied three point calibration data
- Dew Point - measured by a MICHELL Instruments SF52 Dew-Point transmitter and read by MICHELL Instruments Easidew Hygrometer, with voltage logged by TracerDAQ and converted using calibration line from hygrometer readout
- Flow - measured using a Bronkhorst High-Tech B.V. series mass flow meter and logged using the manufacturer supplied software, which is displayed as a percentage of a defined maximum flow for a given gas (here 1.997 g/min air mass flow) and cannot be directly used to measure flow for non-defined components. On this basis it cannot directly determine water vapour flow but it can give an indication of the relative flow between test conditions
- Temperature - measured using Welded Tip Gas and Water Tight PTFE K-type thermocouples fed into the vessel with a Spectite sealed feedthrough supplied by tc.co.uk and logged using a Pico TC-08 datalogger read by Picolog software
- Vessel Band Heater Controller - Watlow EZ Zone Controller

The drying tests were performed to observe common events which occur during drying and the effect of temperature on the drying process. The sample was prepared by first wetting via storage in deionised water for several hours (typically overnight). The rig test temperature was set and once the vessel internal thermocouple read the intended set temperature the sample was prepared and all dataloggers (temperature, pressure, dew point, flow and vessel heater) were started. Prior to testing, the surface water was allowed to run off on the basis that any unbound surface water would simply increase the uncertainty and variability in the sample mass/mass of water, increase the quantity of water removed without demonstrating any technical experimental value and increase the demand on the drying rig for each test. The wet sample was towel dried to a consistent start mass (nominally 14.8 g) to ensure comparability

between tests. The wet sample was loaded into the drying vessel and sealed inside. Then the vessel was evacuated and progress was monitored by observing the live pressure, flow and dew point data. Monitoring the drying was additionally observed by mass loss (accurate to 0.001 g) - assuming all mass loss is attributable to removal of water and no chemical reactions are occurring which would alter the sample mass.

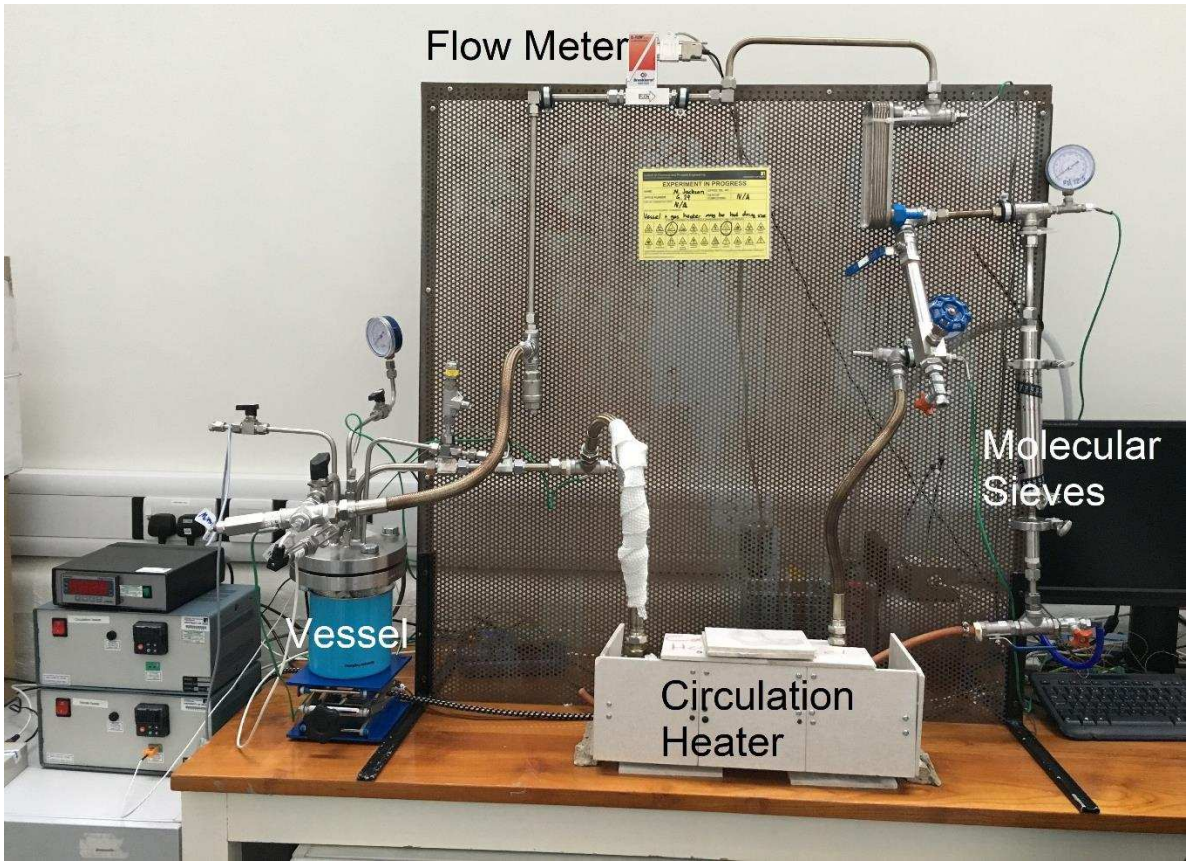

Figure 2. Drying Rig with key components labelled; vessel where samples for drying are placed and sealed, flow meter measures mass flow during drying, molecular sieves hold water vapour from drying, heater used to control circulation gas temperature (flowed gas drying)

RESULTS AND DISCUSSION

TGA and XRD

From the typical magnesium corrosion reaction with water described in Eq. 1 the main product that would be expected in the corrosion product and sludge is magnesium hydroxide. For the mechanically removed corrosion product of Sample 1 this appears to be the case. As shown in the diffractogram in Figure 3a. the only discernible signal is for $Mg(OH)_2$ with the presence of some small and unidentified peaks. For Sample 2 (shown in Figure 3b) which was produced by drying the sludge formed from ultrasonic removal of corrosion product, the XRD shows a mixture of two compounds; magnesium hydroxide, $Mg(OH)_2$ (brucite) and magnesium carbonate hydroxide hydrate, (hydromagnesite) $Mg_5(CO_3)_4(OH)_2(H_2O)_4$. The presence of hydromagnesite/magnesium hydroxycarbonates and compounds other than brucite (such as hydrotalcite, $Mg_6Al_2(CO_3)(OH)_{16}\cdot 4H_2O$) have been identified in real corroded Magnox fuel [6], [14].

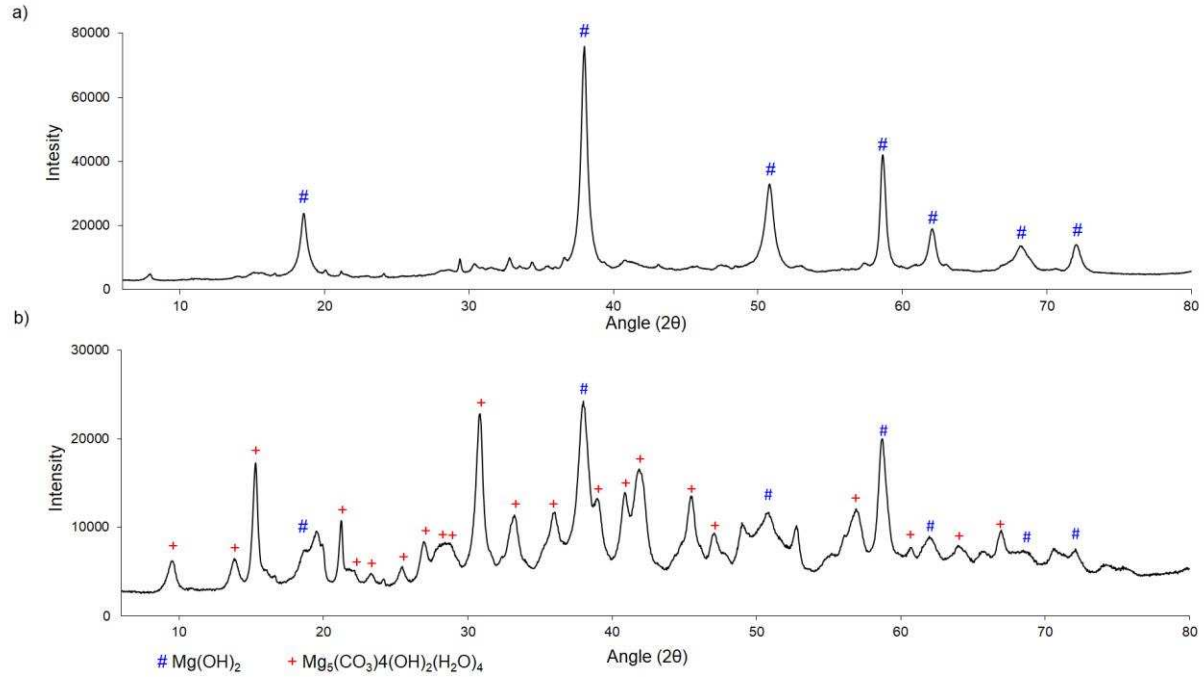

Figure 3. Corroded Magnox XRD; a) Sample 1, b) Sample 2

For Sample 1 and Sample 2 the TGA data is shown in Figure 4. The initial mass of Sample 1 was 19.62 mg, and the final mass was 11.40 mg with an overall mass loss of 8.22 mg (41.9%). The initial mass of Sample 2 was 13.33 mg and the final mass was 11.40 mg with an overall mass loss of 6.4 mg (49.2%), with the data tabulated in Table 1. The mass loss on dehydration of Sample 1 was 9.1%, and 8.3% for Sample 2 the mass loss on dehydroxylation was 23.9% and 7.5%. The mass loss from decarbonation of Sample 2 was 31.4%. As shown by XRD analysis, Sample 1 contained predominantly brucite, whereas Sample 2 contained a mixture of brucite and hydromagnesite. For comparison chemically pure brucite and hydromagnesite are also plotted in Figure 4. The brucite had a total mass loss of 32.8% - less than seen for Sample 1. This is likely to be a result of the initial dehydration up to 280 °C which was greater for Sample 1 by 6.9%. If this difference is subtracted the total mass loss of Sample 1 is closer to that observed for brucite at 35.0%. The hydromagnesite mass loss reached 58.8% - c.f. 49.2% observed for Sample 2. Again, this is expected as a significant proportion of the mass loss is associated with decarbonation, and the mass loss from thermal decomposition of brucite was lower. Sample 2 was seen to contain a mixture of brucite and hydromagnesite, so the resultant mass loss lying between the two is consistent with expectations. Hollingberry and Hull [15] observed a greater mass loss on dehydration and dehydroxylation of hydromagnesite of 15% cf. 15.8%, and a greater loss on decarbonation of 41%% cf. 31.4% for Sample 2.

Table 1. TGA Mass Loss for Corroded Magnox Thermal Decomposition

	Start	Dehydration	Dehydroxylation	Decarbonation	Final
Sample 1					
Mass		17.83	13.15	N/A	11.40
Temperature	19.62	30-280 °C	280-440 °C		800 °C
Mass Loss (Step)		9.1%	23.9%		8.9%
Mass Loss (Total)		9.1%	33.0%		41.9%
$MG(OH)_2$					
Mass (mg)		13.02	9.44	N/A	8.95
Temperature	13.31	30-280 °C	280-440 °C		800 °C
Mass Loss (Step)		2.2%	27.9%		2.7%
Mass Loss (Total)		2.2%	30.1%		32.8%
Sample 2					
Mass		12.22	11.23	7.04.	6.77
Temperature	13.33	30-225 °C	225-330 °C	330-520 °C	800 °C
Mass Loss (Step)		8.3%	7.5%	31.4%	2.03
Mass Loss (Total)		8.3%	15.8%	47.2%	49.2%
Hydromagnesite					
Mass (mg)		9.32	8.29	4.45	4.19
Temperature	10.17	30-225 °C	225-330 °C	330-520 °C	800 °C
Mass Loss (Step)		8.4%	10.2%	37.7%	2.5%
Mass Loss (Total)		8.4%	18.6%	56.3%	58.8%

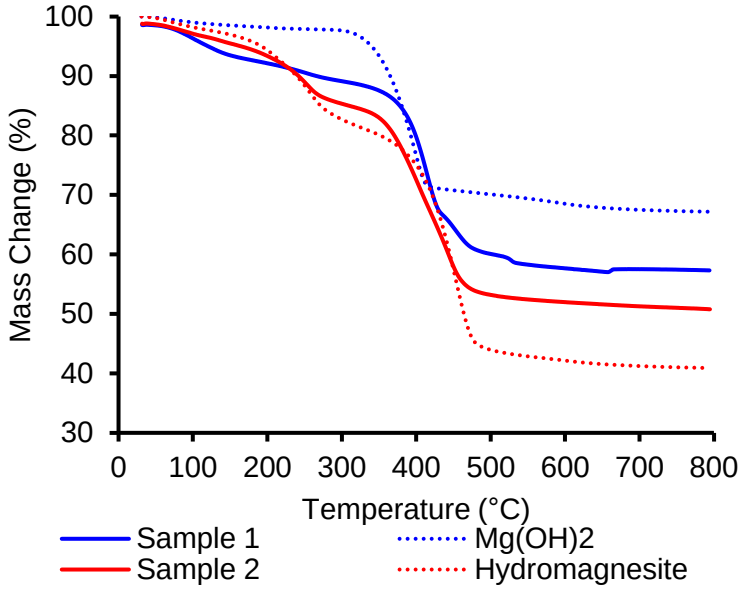

Figure 4. TGA of Corroded Magnox Sample 1, Sample 2, Magnesium Hydroxide and Hydromagnesite

Vacuum Drying

Provided the sample mass is dependent on only dryness/water removal, the rate of mass change should be indicative of the drying rate at each temperature, and the final sample mass loss describes the extent of dryness the test conditions are capable of achieving. Whilst regularly measuring the mass change from drying provides a good assessment of the drying rate, it requires interruption of the experiment as the

vessel must be opened and the sample removed for weighing. This interruption affects the data logger traces, and assumes that sample drying in the period of mass measurement is negligible. In order to display the mass loss clearly it has been overlaid over an uninterrupted test for each set of conditions, but it should be recognised that the mass change data is not from the same set of data shown in the figures.

Figure 5 shows the drying data for all tests undertaken at 40 °C, 60 °C, 90 °C and 120 °C. As mentioned, the mass change data has been plotted over an uninterrupted single run as an indication of the sample mass change (i.e. water removal) over time and the corresponding flow, pressure and dew point. At the 180 min and 250 min points on Figure 5b-d are points that the vessel was opened to inspect and weigh the sample, which gives rise to the sudden increase in flow and pressure. As such, these sections in the plots can be ignored and do not display any meaningful data. Also it can be seen that these interruptions do not seem to have a significant impact or effect on the drying process as the pressure, dew point and flow all resume the level observed before the interruption once it has stabilised. For all tests the majority of the drying occurs within the first 90 mins, so all data from Figure 5 have been replotted on a 0-90 min scale in Figure 6 for clarity.

As can be seen in Figure 6, the pressure, dew point and flow show very good agreement in relationship. At 40 °C the traces remain steady for 45 mins (pressure = 28 mbar, dew point = 23 °C and flow = 2.2%), followed by steady decrease until 75 mins. Then all three levels are low and flow/pressure/dew point change slows further, eventually levelling off after 120 mins. The pressure and flow both plateau and remain steady (at 4-5 mbar and 0.06% respectively) for the remaining time up to 270 mins. The dew point continues to slowly decrease with time even once the pressure and flow remain constant, eventually reaching -16 °C at 270 mins. The mass change shows a similar relationship, steadily decreasing from 0 to 60 mins. The rate of mass loss decreases after this point, but there is some gradual mass loss from 90 minutes onwards. The temperature drops initially to 31 °C on vessel evacuation due to adiabatic cooling, where it remains until t = ~30 mins. From 30 mins onwards the temperature begins to rise steadily to 45 °C at t = ~115 mins where it remains for the rest of the test. Following the initial drying period and adiabatic cooling the heater caused the temperature to increase above the set temperature which is not intended. Also the temperature trace shows a visible undulating pattern which is an artefact of the cyclical heating application and cooling from the vessel heater and is not related to the drying process or testing.

The tests at 60-120 °C show very similar drying behaviour with some resemblances and differences from that observed at 40 °C. As with the 40 °C test, the pressure, dew point and flow data all show a close relationship. For all tests, the pressure, dew point and flow stay at a steady level until 60-70 mins has passed, where all levels drop significantly and suddenly, and by 75-90 mins all pressure and flow has flattened to <6.5 mbar and <0.1% respectively. As with the 40 °C test, the dew point at the 60-120 °C tests also continues to decrease even once the pressure and flows have plateaued. The dew point at the 180 min mark where the process was interrupted for sample inspection are -11, -15 and -25 °C at 60, 90 and 120 °C respectively. As expected, the mass loss is more rapid with increasing temperature. At 40 °C the mass showed steady consistent loss for 90 mins of drying, whereas consistent mass loss was no longer observable after 60 mins at 60 °C, ~30 mins at 90 °C and 20 mins at 120 °C. As seen at 40 °C, the initial period after evacuation is associated with a temperature drop for all tests from adiabatic cooling, but also following this period the temperature went on to exceed the set temperature. The 60 °C test actually reached 70 °C after 70 mins of drying. For the 90 °C the temperature reached 107 °C after 35 mins. This was noticed and manual attempts to reduce the heater set temperature were made to reduce the vessel internal temperature, eventually bringing it down to 94 °C 110 mins into drying. For the 120 °C test the temperature rose to 138 °C after 30 mins of drying. Again, this was noticed and the vessel temperature was manually brought down to 120 °C by 50 mins into the test. These temperature variations are a result of operation limitations of the vessel band heater controller and not an artefact of the drying process.

The average water loading and subsequent mass loss for all samples was 1.69 g. The mass changes during drying are plotted for comparison in Figure 7a, which is rescaled to include only the first 90 mins of data in Figure 7b for clarity. As previously discussed, the initial drying rate increases with increasing temperature. As the figures and table show, after the initial bulk of the water has been removed in the first 90 mins, prolonged drying does give rise to further mass loss. Assuming this mass loss is attributable to removal of water, this implies that the corroded Magnox does retain water which is harder to remove than surface water. Furthermore, it became evident during sample observations that following removal from the vessel the mass of dried sample would steadily increase. This is presumed to be from either absorption of water vapour from the atmosphere, or potentially a chemical reaction with atmospheric oxygen/water. As this mass gain was reversible following further drying, it can be assumed this is not due to oxidation in air as the reduction would not be achievable at these conditions. To investigate this further, following a 5 hour drying test undertaken at 40 °C the sample was held on a balance in the open and the mass was observed over time. The results are shown in Figure 8, which demonstrate that the sample mass increased from 13.268 g by 36 mg to 13.304 g over 30 mins, and then by a total of 119 mg to a mass of 13.387 g when left for four days. Assuming this effect is due to the reabsorption of water vapour following drying, this could have implications on the way Magnox Spent Fuel is handled following drying in storage.

The extended drying tests also show that the final dry sample mass was lower with increasing temperature from 40-90 °C, despite each test being performed using the same sample each time. Interestingly this trend was not observed to the same effect at 120 °C. The average final mass at 40, 60, 90 and at 120 °C was 13.225, 13.132, 13.102 and 13.134 respectively - the 120 °C average final mass being 32 mg greater than that observed at 90 °C It is acknowledged that not all of these tests were performed for the same length of time but the trend does appear to be clear, and is visible in Figure 7b. In the first 20 minutes the 120 °C test has the most rapid and rate of mass loss and lowest mass, but as time progresses the 90 °C test dry sample has the lower mass. At 60 minutes the 90 °C tests have an average sample mass of 13.144 g, which goes down to 13.121 g after 120 minutes, compared to 120 °C which averages 13.154 g (11 mg more) and 13.141 g (20 mg more). The difference between the 90 °C and 120 °C mass change suggests that not only does increasing the temperature increase the drying rate for water in corroded Magnox, but also the total amount of water that can be removed - provided the temperature is not too great. The reason for this has not been investigated, but perhaps the higher temperatures cause water vapour/surface water to react with the magnesium cladding. Friskney et Al. describe that the post breakaway rate increases by two orders of magnitude with an increase of temperature from 70-120 °C in pH 11.5 sodium hydroxide solution [7]. In that case, during the drying process employed here the sample is presumably in contact with heated water/water vapour in the initial period of drying before the bulk of the water has been removed and any metal in contact with this water is free to react. As such it is possible that the heating and water vapour is causing the Magnox to corrode at the highest temperatures before the water itself is removed. Further investigation into this effect could be measured by undertaking tests to observe how Magnox/magnesium reacts with heated water vapour/water at reduced pressure (<50 mbar).

It is noteworthy that the mass change trend does not follow the same shape as the pressure/flow data for the tests at 60-120 °C. In the 40 °C tests, the mass loss is steady and appears to follow the same trend as the pressure and flow data. At 60 °C and above, the mass loss is more rapid, especially in the first 30 minutes of drying, but this is not represented in the flow or pressure data. If the pressure/flow level was directly related to the mass loss it would be expected that the flow and pressure would be significantly greater during this period of greatest rate of mass loss. On this basis, it can be inferred that the sample surface water vaporises relatively quickly but there is an extended period following the vaporisation where the gaseous water is slowly removed, causing the delayed pressure and flow reduction and limited by the rig setup and performance.

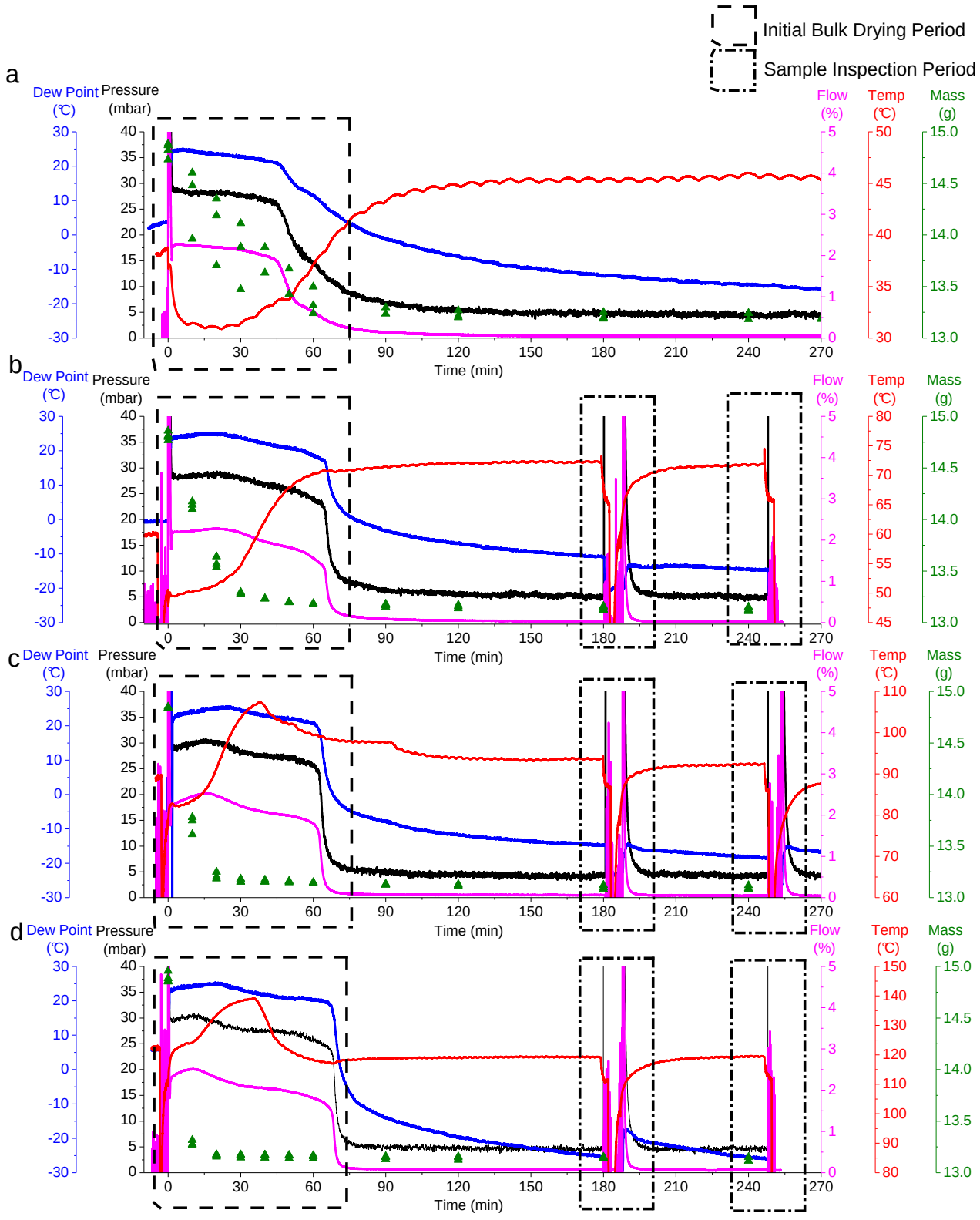

Figure 5. Pressure, Dew Point, Flow, Temperature and Mass Change during Drying at a) 40 °C, b) 60 °C, c) 90 °C, d) 120 °C

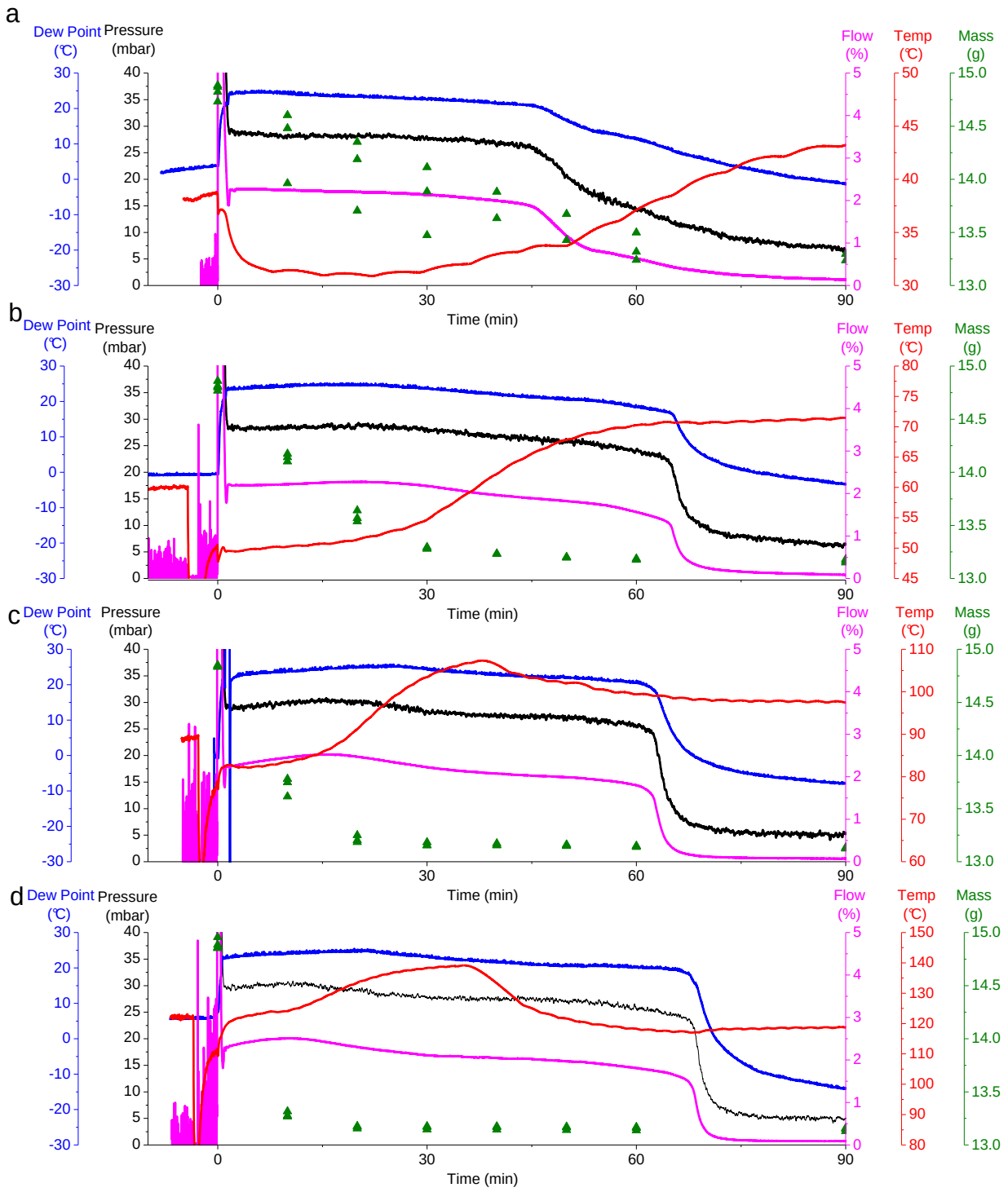

Figure 6. Pressure, Dew Point, Flow, Temperature and Mass Change during First 90 mins of Drying at a) 40 °C, b) 60 °C, c) 90 °C, d) 120 °C

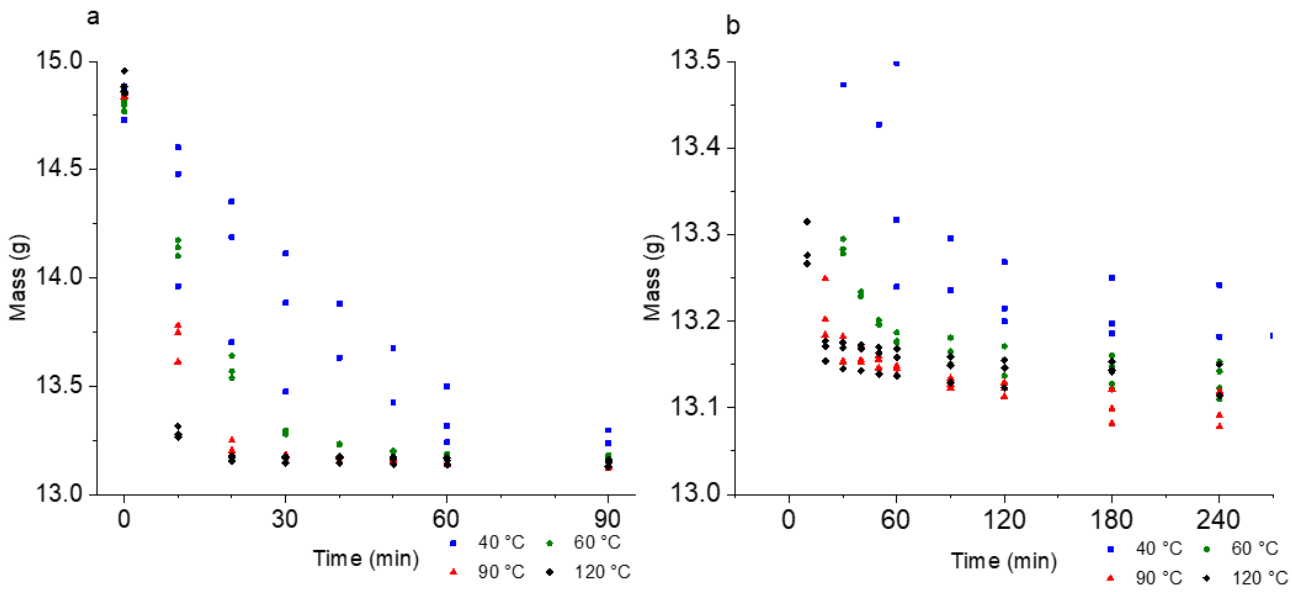

Figure 7. Sample Mass Loss during Drying; a) Initial 90 min Duration b) 360 min Duration (note different y-axis mass scale)

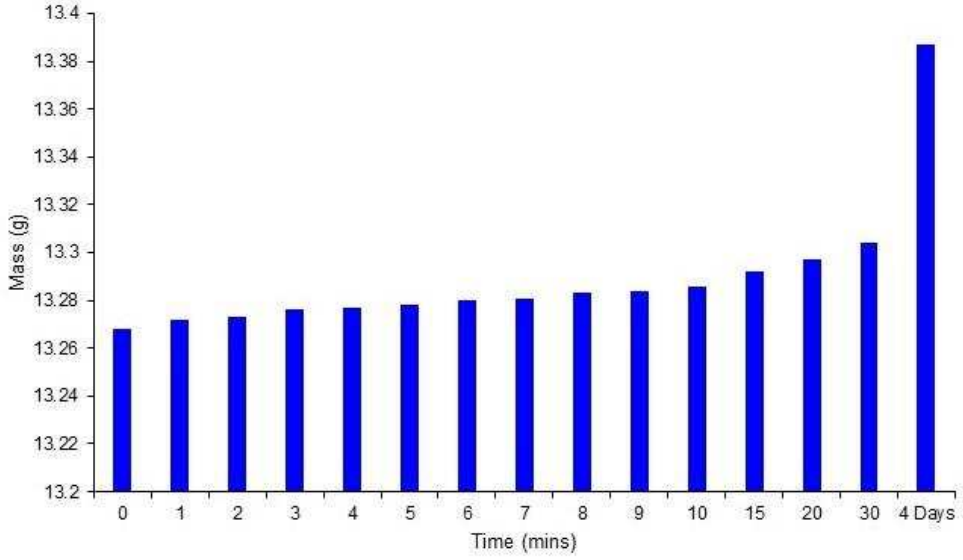

Figure 8. Sample Mass Change Following 5 h Drying at 40 °C

Conditions during Drying

All the pressure and flow data shown in Figure 6 appear to have the same relationship. At 40 °C the flow and pressure were initially the same for the first 45 minutes at 28 mbar pressure and 2.2% flow. After this point both sets of data drop gradually. This suggests that at 40 °C there could be some interactions between the sample surface and chemically or physically bound water which is slower to remove. At 60-120 °C this gradual water loss is not visible. At these temperatures the general shape of the pressure and flow traces are very similar. The pressure/flow remain roughly constant for 60-70 minutes where it drops suddenly. When the pressure and flow drop like this, it can be presumed that the water vapour has been removed and is no longer forming, indicating the point of dryness.

From the available live and in situ measurements available during drying, the pressure and flow appear to give an indication of the quantity of water that has been removed over time, and helps to detect the point that dryness is achieved by means of a sharp drop in pressure/flow. The dew point meter also provides an insight to the drying progress but is less conclusive for indicating when the sample is nominally dry as the dew point tends to gradually continue to decrease for an extended period following the indicated point of dryness.

CONCLUSIONS

Drying rig testing and corroded Magnox characterisation have been carried out and completed. This is summarised as follows:

1. A rig capable of performing drying at reduced pressure <4 mbar is operable for performing drying tests to support the investigation.
2. Inactive simulant corroded Magnox samples have been acquired and are readily available from NNL. Initial testing and characterisation have been performed upon these including:
    a. Corrosion product removal by ultrasonic bath and sludge isolation/drying.
    b. Powder XRD performed on corrosion product and sludge from two samples, identifying magnesium hydroxide as the main corrosion product, but also identifying other magnesium carbonate hydroxide hydrate (hydromagnesite), showing that the sludge and corrosion products may contain chemically bound water.
    c. TGA was performed on two samples to quantify the water and other species present in the corroded Magnox, and was observed to be 9.1% water 23.9% hydroxide in one sample, and the second sample analysed as 8.3% water, 7.5% hydroxide and 31.4% carbonate by mass - evidence that the corrosion product is ~10% water by mass.
3. Vacuum drying has been performed on wet corroded Magnox at 40, 60, 90 and 120 °C. To monitor the process, vessel pressure, dew point, flow, temperature and sample mass were measured. The results of this data have yielded the following conclusions:
    a. Increasing the temperature increases the initial drying rate. At 40 °C the majority of the mass loss from removal of 1.7 g of water was observed to be gradual and over 90 minutes, which was reduced to 60 minutes at 60 °C, 30 mins at 90 °C and 12 mins at 90 °C. Also increasing the temperature causes a greater mass loss between 40-90 °C. At 120 °C the final sample mass was greater after 5 hours drying than at 90 °C. It is suggested that the increase in temperature is causing the sample to react with the water/vapour during the drying process.
    b. Extended drying times (> 2 hours) gave rise to very gradual further sample mass loss despite the instrumentation detecting no significant quantities of pressure or flow.
    c. Following the drying tests, the Magnox sample was observed to slowly gain mass while exposed to the open atmosphere. After five hours vacuum drying at 40 °C, the sample was seen to increase in mass from 13.268 g to 13.304 g over a 30 minute period, which then continued to rise to 13.387 after four days. This mass change may be attributable to the dried sample absorbing water from the atmosphere, which could have implications for storage of spent Magnox fuel following drying.
    d. At 40 °C the rate of drying appears to be slower and more gradual than at ≥60 °C. At 40 °C all data traces reduce over a period of ~45 minutes until the conditions appear stable and nominally dry. At ≥60 °C the drying period is shorter and the point of dryness appears to be sudden and abrupt, where the mass of water quickly declines, then following a delay of 30-50 minutes the pressure and flow abruptly drop to a stable state indicating the sample and vessel conditions are nominally dry.
    e. The pressure and flow have an almost identical relationship over the course of a drying test. During drying, both showed steady traces with the pressure at ~28 mbar and the flow

at 2.2%. Once the conditions appeared dry the pressure would stay at <6.5 mbar and the flow at <0.1%. Both pressure and flow on this basis provide good non-invasive indication as to the progress of the drying test, and have been able to establish a point of dryness/completion of bulk sample drying.

f. The dew point provides an alternative non-invasive indication of the conditions within the vessel and can also inform the progress of the drying test. The general trend of the dew point is very similar to that of the pressure and flow. It is higher during initial drying (20-25 °C) which drops suddenly as the water vapour is removed, but unlike the pressure and flow which stabilise relatively quickly following the point of nominal dryness, when a sample is present the dew point would gradually decrease over time. The reasons for this are not yet fully understood, but it suggests that the dew point meter may be more sensitive to any slow release of water held within the sample which is not observable by the pressure transducer and flow meter. As such the dew point meter provides useful additional information to the drying progress but is harder for determining the point of dryness.

g. The vessel band heater that controls the temperature is known to overheat the vessel and this is believed to be the biggest source of inconsistency in the tests. Manual attempts to accommodate for the lack of precision on the temperature control have been made as much as possible but some temperature excursions have been observed. The effects of these are not believed to be significant as the excursions have occurred after the period of greatest sample drying.

REFERENCES

[1] C. Hinton, “Calder Hall,” J. Nucl. Energy, vol. 4, no. 1, pp. 1-IN1, 1957.

[2] E. and I. S. Department for Business, “Uk Energy in Brief 2018,” 2018.

[3] EDF Energy, “Where are EDF Energy’s nuclear power stations located in the UK?” [Online]. Available: https://edfenergyuk.custhelp.com/app/answers/detail/a_id/843/~/where-are-edf-energys-nuclear-power-stations-located-in-the-uk%3F. [Accessed: 01-Jul-2019].

[4] Pöyry Energy Limited and Amec Foster Wheeler plc., “Radioactive Waste Inventory: Radioactive wastes and materials not reported in the 2016 Waste Inventory,” 2017.

[5] IAEA, “Spent Fuel Performance Assessment and Research: Final Report of a Coordinated Research Project (SPAR-II),” 2012.

[6] C. R. Gregson, D. T. Goddard, M. J. Sarsfield, and R. J. Taylor, “Combined electron microscopy and vibrational spectroscopy study of corroded Magnox sludge from a legacy spent nuclear fuel storage pond,” J. Nucl. Mater., vol. 412, no. 1, pp. 145–156, May 2011.

[7] C. Friskney et al., “The corrosion of Magnox Al-80 alloy in aqueous and moist environments BSc, PhD (now at CEGB SE Region Scientific Services Department), and P.M. BRADFORD, BSc (now with the Nuclear Installations Inspectorate).”

[8] J. Morris, S. Wickham, P. Richardson, C. Rhodes, and M. Newland, “Contingency Options for the Drying, Conditioning and Packaging of Magnox Spent Fuel in the UK, ICEM2009-16331,” 2017.

[9] J. E. Morris, P. J. Richardson, and S. M. Wickham, “Magnox Spent Fuel Contingency: Review of Options for Drying, Packaging and Storage of Magnox Fuel (Unpublished),” 2009.

[10] Office for Nuclear Regulation, “Review of Magnox Reprocessing Separation Plant Regulatory Strategy - ONR-SEL-PAR-15-004,” pp. 1–12, 2015.

[11] ASTM C1553-16, Standard Guide for Drying Behavior of Spent Nuclear Fuel. West Conshohocken, PA: ASTM International, 2016.

[12] J. B. Goode, D. I. Hambley, and B. C. Hanson, “End point determination for spent nuclear fuel drying operations,” Prog. Nucl. Energy, vol. 116, pp. 108–114, 2019.

[13] J. B. Goode, D. Harbottle, and B. C. Hanson, “Vacuum drying of advanced gas reactor fuel,” Prog. Nucl. Energy, vol. 109, pp. 145–158, 2018.

[14] K. R. Hallam, P. C. Minshall, P. J. Heard, and P. E. Flewitt, “Corrosion of the alloys Magnox AL80, Magnox ZR55 and pure magnesium in air containing water vapour,” Corros. Sci., vol. 112, pp. 347–363, 2016.

[15] L. A. Hollingbery and T. R. Hull, “The thermal decomposition of natural mixtures of huntite and hydromagnesite,” Thermochim. Acta, vol. 528, pp. 45–52, Jan. 2012.

ACKNOWLEDGEMENTS

Thanks to the Engineering and Physical Sciences Research Council (EPSRC) and Nuclear Decommissioning Authority for funding this work through the Next Generation Nuclear Centre for Doctoral Training (NGN CDT). Thanks also to Dr James Goode at the National Nuclear Laboratory, Martyn Barnes from Sellafield Ltd, and to Chris Bulman, Bob Harris, Karine Alves Thorne, Dr Adrian Cunliffe and Dr Faye Esat at the University of Leeds.